学位申請論文

小山 勝二

~~$^{12}C(\tau, d)^{13}N$ Reaction~~

^{12}C (τ, d)^{13}N Reaction at 81.4 MeV

Katsuji KOYAMA

Institute for Nuclear Study, University of Tokyo,
Tanashi, Tokyo

(Received)

Abstract

The $^{12}C(\tau, d)^{13}N$ reaction was investigated at an incident energy of 81.4 MeV. Angular distributions of the reaction were analyzed by zero-range and finite-range DWBA. It is found that finite-range effects are important in this reaction. Particle unbound states are analyzed by using resonant form factors, and the results are discussed in comparison with those of proton resonance scattering.

Present address: Institute of Space and Aeronautical Science,
University of Tokyo, Meguro, Tokyo

§ 1. Introduction

The reaction $^{12}C(\tau,d)^{13}N$ has been studied thus far by several authors over the range from 12 MeV to 25 MeV[1], and it has been found that the reaction can be reproduced in the frame-work of zero-range (ZR)DWBA in the range of the bombarding energy from 16 to 18 MeV. In these analyses the particle unbound states have been also studied by using resonance form factors.

It is interesting to investigate the reaction mechanism at higher incident energies. It is considered that finite range effects become important even in the light ion reactions[2] when the incident energy and hence the momentum mismatching increases. These effects are approximately included by local energy approximation (LEA)[3] which has been successfully applied to the incident energy around 40 MeV[4]. In that energy region, however, finite-range effects are not so large and the difference between ZR and LEA is not significant. H.Doubri et al.[5] studied the (d,τ) reaction at 82 MeV, and found that the reaction can be well explained in terms of LEA. In the present paper, the importance of the effects of the finite range in the reaction $^{12}C(\tau,d)^{13}N$ at 81.4 MeV is demonstrated. The reaction mechanism to the unbound states is also discussed.

It is considered that even in the unbound state, usual DWBA theory is still a useful tool for the case of small width. However, the form factor oscillates in sign and decreases slowly in magnitude with increasing radius. We must therefore introduce some practical methods to the numerical integration. Huby and Mines[6] used a convergence

factor $e^{-\alpha r}$ in the integrand and extrapolated the result to the limit $\alpha \to 0$. Vincent and Fortune[7] employed very ingenious method, in which the radial integration was carried out in complex r - plane instead of real radius. At present, this is the most useful method for the analysis of the resonance state.

Determination of the form factor has always been the problem for nuclear spectroscopy with direct reactions. Usually the form factor is determined by separation energy method. For the unbound state, the form factor can be compared with actual scattering wave function which is experimentally obtained by the corresponding resonance scattering, so that the ambiguity of the form factor could be small. The spectroscopic factor deduced from the transfer reaction is compared with the single particle width obtained from the resonance scattering.

In section 2, experimental procedures are described. In section 3-1. the effects of finite-range and non-locality are discussed. In section 3-2 the analysis with the resonance form factors is presented. The results are summarized in section 4.

§ 2. Experimental Procedure

The ion beam of doubly charged ^{3}He at 81.4 MeV from the synchro-cyclotron at Institute for Nuclear Study, University of Tokyo, was momentum analyzed by a beam analyzer magnet to 0.1 % accuracy, and was transported to the target chamber through a cleaning magnet and Q-magnets. The beam intensity at the target was 1~2 nA in a bunched beam.

The target was a natural carbon foil of thickness 5.64mg/cm^2 which was prepared by a method of thermal cracking of methane gas. The reaction products were detected with the INS magnetic analyzer system[8]. The position signals were obtained by an array of proportional counters placed at the focal plane. The particle identification was provided by the energy signals from plastic scintillation counters placed behind the array of proportional counters. The position signals were fed into the PDP-9 computer to obtain deuteron spectrum. At the end of each run, the spectrum obtained was transferred to the central computer TOSBAC-3400 and processed with on-line programs[9].

The mesurements were carried out at various angles between 6° and 40° in 2° steps and between 40° and 60° in 2.5° steps. In order to avoid the kinematical energy spread, the acceptance angle of the spectrometer was limited as small as 0.4° . The over-all energy resolution was about 300 keV(FWHM) mainly due to the energy loss in the target and the kinematical spread.

A typical energy spectrum is shown in fig.1. Except for the ground state, all the states are particle unbound states. Some prominent peaks are observed above the background which is mainly due to the three body break up and the cross sections of unbound states were obtained after substracting this continuous back ground part. The peaks at 2.37 MeV and 3.55 MeV (doublet with 3.51 MeV) are s1/2 and d5/2 single particle states, respectively. The broad bump near 8 MeV is considered due to the d3/2 single particle resonance. The peak at 10.4 MeV corresponds to $7/2^-$ — $5/2^-$ doublet state. The peaks near 11.1 and 12.1 MeV are considered to be $5/2^-$ and $7/2^-$ states, respectively[10].

3. Result and Analysis

3-1 DWBA calculations using bound state form factors.

The DWBA analysis was carried out for the ground state, 2.37-MeV state and 3.55 MeV state. For the 2.37-and 3.55-MeV states, loosely bound form factors for binding energy 0.05 MeV were used. The 3.55 MeV state is a doublet with 3.51-MeV. Since the single particle width of the 3.55-MeV state is about seven times larger than that of the 3.51-MeV state[10], the 3.55-MeV state only was considered.

The calculations were carried out in the frame-work of zero-range DWBA, zero-range DWBA with finite range correction by means of local energy approximation using the code DWUCK[11], and exact finite-range DWBA using the code INS-DWBA4[12]. These calculations were performed with the TOSBAC-3400 computer at Institute for Nuclear Study (INS). The results of the calculations are shown in fig.2 with the following designations together with the experimental data; ZR-L(zero-range calculation using local potential), ZR-NL(zero-range calculation using non-local potential), LEA-NL(finite-range correction using non-local potential), and FR-NL (exact finite-range calculation using non-local potential). The non-locality parameters for ^{3}He and for deuteron were assumed to be 0.25 and 0.54, respectively, which are the conventional values. The finite-range parameter of LEA was taken to be 0.77 (in DWUCK). In the calculation for exact finite-range, the interaction between deuteron and proton was assumed to be of guassian form,

$$V(r) = V_0 \exp(-r^2/\xi^2)$$

where the range parameter was taken to be 2.0fm which gives a reasonable radius of ^{3}He obtained from the electron scattering experiment[13].

The distorting potential used has a form

$$V(r) = V_C(r_C) - V_0 f(x_0) + (\hbar/m_\pi c)^2 V_S \, (1 \cdot \vec{\sigma}) \, 1/r \, \frac{d}{dr} f(x_S) + iW_D \frac{d}{dr} f(x_D) \ ,$$

where $f(x') = (1+e^{x'})^{-1}$, $x' = (r - r'A^{1/3})/a$,

and $V_c(r_c)$ is the Coulomb potential of a uniformly charged sphere of radius $r_c A^{1/3}$.

The potential parameters of deuteron were substituted by the ^{12}C + d potential of ref.14), and those of ^{3}He were determined from the elastic scattering on ^{12}C at 82.1 MeV[15], (see fig.3). All these parameters are summarized in Table 1. In the present calculations, the potential set.1 in the Table was used. The binding potential of a proton was a usual one.

Since there exist some ambiguties in deuteron optical potential, its influence was examined by changing the real part V_o and the imaginary part W_D in ZR-DWBA. When V_o is reduced to as small as 50 MeV, the fit to the ground state (p1/2) and the 2.37-MeV (s1/2) state improves only slightly. On the other hand the fit for the 3.55-MeV (d5/2) state becomes worse. When W_D was varied, no significant improvement was observed for all the states.

There remains also some ambiguity in determining the form factor. When the proton real radius parameter r_0 is increased to 1.4fm, a little improvement was obtained for the p1/2 state, but not for the s1/2 and the d5/2 states.

The real radius of the optical potential of ^{3}He of set.1 may be somewhat too small. If we use the optical potential set.2, in which a larger radius (r = 1.2fm) is assumed, the DWBA result gives better fit to the p1/2 state only. However, this optical potential set yields considerably poor fit to the observed elastic scattering data compared with the former one at backward angles (see Fig.3).

As the result, a slight improvement is obtainable only for the p1/2 state by a reasonable change of potential parameters, but for the s1/2 and the d5/2 states almost no significant effect is observed. Thus, we consider that the potential sets employed in the present calculation is an appropriate one.

3-2 The DWBA calculations using resonance form factor.

For the resonance state, the DWBA calculation was performed in the frame-work of ZR-L and LEA-NL with the same potential as that of section 3-1. As seen in section (3.1) (see fig.2), the LEA provides a good approximation for the calculation with bound state form factor. We therefore employed LEA also for the case with resonance form factor.

The DWBA calculation was performed by the method of Vincent and Fortune[7] using the code INS-DWBA2[16] with FACOM 360-75 computer at the Institute of Physical and Chemical Reserch (IPCR). The integration was carried out along real axis from 0 fm to r_t fm in 0.1 fm step and then proceeded along a line parallel to the imaginary axis with the same step.

In the present calculation, r_t was taken to be 14-20 fm. The results are shown in fig.4 by ~~dotted~~ dashed (ZR-L) and solid (LEA-NL) curves.

For the form factors of the 2.37-MeV (s1/2) and 3.55-MeV (d5/2) states, we used so called Gamow functions[17] with complex eigen value $E_R - i\Gamma/2$, where E_R and Γ are the resonance energy and width, respectively. As an example, the resonance form factor of s1/2 is shown in fig.5 together with the loosly bound form factor.

The potential was determined so as to reproduce the experimental resonance energies. The geometry of this potential and the strength of the spin-orbit term V_S were assumed to be equal to the case of loosely bound form factors (see Table 1), and the imaginary part was taken to be zero. Then the real part of this potential is expressed by

$$V = 59 - 0.25E \text{ (MeV)}$$

As shown in fig.6, this potential reproduces fairly well the observed elastic scattering of low-energy protons on ^{12}C off resonance energy when inelastic channel is not appreciable (below $E_p = \sim 7$ MeV).

3-3 The results for higher excited states.

The experimental results for other states than the ground (p1/2) state, 2.37-MeV (s1/2) and 3.55-MeV (d5/2) states are given in fig.7. The 7.9 MeV ($3/2^+$) state is considered to be a d3/2 single-particle resonance state having a width of 1.72 MeV. In spite of such a large width,

the angular distribution is very similar to that of the d5/2 state at 3.55 MeV which has much smaller width.

The 7.2 — 7.4 MeV states are considered to be a $7/2^+$ — $5/2^-$ doublet[10]. It is noticeable that the angular distribution of these two states is flatter than that of the other states.

The 10.4 MeV peak corresponds to the states strongly excited by proton resonance scattering at E_p = 9.13 — 9.15 MeV. This peak is considered to be a $7/2^-$ — $5/2^-$ doublet, each of which has a rather small single particle width[10]. The reason for the relatively strong excitation of these states is the angular momentum mismatching which suppresses the low spin states. In this case the difference of the angular momentum between the incident wave and the outgoing wave at the nuclear surface is about three. At the lower incident energy where angular momentum mismatching is small such as observed at 29.3 MeV, this state is not so strongly excited.

Near the peaks at 11.1 and 12.08 MeV, there are many levels such as $5/2^+$, $5/2^-$, $3/2^+$, $3/2^-$, $1/2^+$ and $7/2^-$, all having small single particle widths[10]. The appearance of the two relatively strong peaks suggests an exsistence of high spin states. The angular distributions for these states are very similar to that of the 10.4 MeV states, suggesting that these levels are also $5/2^-$ and/or $7/2^-$ states.

4. Discussion

4-1 Angular distribution

Main featurers of the result of the present analysis are summarized as follows;

(1) Conventional zero-range local DWBA calculations cannot give overall fits to the observed angular distributions, and finite-range effect is found to be significant in the present energy region. The LEA is shown to be a good approximation to the exact finite-range calculation even at such a high incident energy as 81.4 MeV. The finite range effect reduces the contribution of the inner part of the form factor, which eventually suppresses the lower partial wave components. This effect becomes large with increasing incident energy and increasing momentum mismatching. The correction for the potential non-locality yields a better fit as the result of the same effect. (Fig.2)

(2) The resonance form factor is better than loosely bound form factor in order to reproduce the angular distribution of the unbound state. The resonance form factor well reproduces the second hump for the s1/2 state, whereas it smears out the structure which is otherwise produced in the angular distribution for the d5/2 in comparison with the observed result. Resonance form factor gives similar result for the cases of finite-range and potential non-locality. (Fig.2) This is considered to be due to the effect that the resonance form factor decreases slowly with increasing radius, and that the contribution of higher partial waves is larger than the case of loosely bound form factor. (Fig.4)

(3) Although considerable improvement is obtained by including above-mentioned effects, the overall fits are not very satisfactory.

Phenomenologically speaking, very large non-localities of the optical potential give very good fits to all the states. This situation is very similar to those of (d,p) and (p,d) reactions at considerably high incident energy[18].

The physical meaning of this large non-locality is still not clear. One possible case may be to take into account a coupled channel effect. In our reaction, the inelastic channel of ^{3}He on $^{12}C(4.43\ MeV\ 2^{+})$ is very large[15] so that the coupled channel effect may be important. For example, the two step process via an inelastic channel is of the order of about one-tenth of the direct process. However the ground (P1/2) state and the 3.55-MeV state (d5/2) are mainly single particle states and are excited strongly. Therefore, the two step precess would be negligible for these states. The 2.37 MeV (s1/2) state is usually considered as mainly single particle state also. On the other hand, it is shown that the differential cross section for the s1/2 in heavy ion reactions is well reproduced by the coupled channel calculation in which a large admixture of core excited state is assumed for the description of this state[19]. We estimated the contribution of two-step process using the form factor including the core excited state, but obtained no improvement.

4-2 Spectroscopic factor

The spectroscopic factors obtained from various cases shown in fig.2 and fig.4 are listed in Table II together with those obtained from low incident energy[1] and resonance reactions[10]. As shown in Table II, the spectroscopic factors obtained from resonance form factors are slightly larger than those from loosely bound form factors.

LEA gives smaller spectroscopic factors than FR. We used the normalization factor $D_0^2 = 2.99 \times 10^4$ MeV$^2 \cdot$ F^3 according to Bassel[4].

For the ground state, the spectroscopic factor obtained is 0.78 for FR. This value is a little larger than the value predicted by Cohen and Kurath (0.66). The spectroscopic factors obtained for lower incident energies and that of analogue state obtained from the reaction $^{12}C(d,p)^{13}C$ at a low incident energy[20] are considerably larger than the value of Cohen and Kurath. As is suggested in ref.1, such large values may be due to the resonances in $^{12}C + \tau$ and $^{12}C + d$ systems. Since the resonance effect is very small at 81.4 MeV, our value should be more reliable.

For the s1/2 state, the spectroscopic factor obtained from ZR calculation is too small to fit the experimental data. The LEA calculation using the resonance form factor gives a value of 0.15, which is somewhat smaller than that derived from the case of low incident energy. This value is considerably smaller than the value of reduced width $\theta_p^2 = 0.54$ obtained from proton elastic scattering.

For the d5/2 state, the spectroscopic factor obtained from LEA with the resonance form factor is 0.87, which is much larger than the experimental value of $\theta_p^2 = 0.21$. This is quite opposite to the case of s1/2.

In conclusion, the spectroscopic factor obtained from the present experiment is reasonable for the ground state. For unbound states, these values do not agree with the values of θ_p^2. As pointed out in ref.1, more accurate calculation of penetrability, in which the potential

scattering is correctly accounted for, gives much smaller reduced width[1]. Therefore an agreement for the s1/2 state may be improved. On the other hand, according to the shell model calculations by T.Sebe[23], the spectroscopic factors for the s1/2 and the d5/2 states are as large as 0.92 and 0.83, respectively. The coupled channel calculation of low energy ^{12}C + p scattering[24] also gives large spectroscopic factors for these states. They are 0.92 and 0.72 for the s1/2 and the d5/2 states, respectively.

For the d5/2 state these large values are consistent to the value obtained from our measurement, whereas for the s1/2 state our result is too small compared with the theoretical values.

At the present stage, it is not possible yet to determine correct values of the spectroscopic factors. In order to provide further consistency check on the spectroscopic factors obtained from the two types of measurements (resonance reactions and the direct reaction), it is necessary to study the stripping reaction to unbound states more extensively for various targets and for a wide range of incident energy.

Acknowledgements

The author would like to thank Professors S.Kobayashi, H.Ohnuma, and Y.Hirao for their interest and encouragement throughout the work. He also thanks Drs. T.Tanabe, M.Yasue, Y.Ishizaki, H.Yokomizo, T.Hasegawa, M.Tanaka, K.Ogino, H.Sakaguchi, S.Tanaka, A.Goto, Y.Toba and N.Koori for their helpful cooperation, and M.Igarashi and N.Nakanishi for valuable discussions. He wishes to express his thanks to professor Kuntz for the use of DWUCK, and Professor H.Yoshida for the use of DWBA-4.

Figure Captions

Fig. 1. A typical energy spectrum of deuterons at 7^{o}.

Fig. 2. Comparison of DWBA calculations with the expermental data.
For ^{3}He the potential set 1 is used.
The dotted curves (- - - -) are the results of ZR-L, dashed curve (– – –) are ZR-NL, solid curve (———) are LEA-NL, and dott-dashed curve (– · – ·) are FR-NL.

Fig. 3. Angular distribution for elastic scattering of ^{3}He on ^{12}C at 82.1 MeV. The curves are the results of optical model calculations.

Fig. 4. The DWBA calculations using resonance form factors together with expermental data.
The dashed curves (– – –) are the results of ZR-L and solid curves (———) are LEA-NL. The DWBA calculations using loosely bound form factors are given by dotted curves (- - - -) for comparison.

Fig. 5. The form factors of $s^{1/2}$ state. The solid curve (———) and dotted curve (- - - -) are real part and imaginary part of resonance form factor, respectively. The dashed curve (– – –) is loosely bound form factor.

Fig. 6. The optical model calculations of low energy proton elastic scattering on ^{12}C. The experimental data at E_p = 4.66 MeV are taken from ref.21, and those at E_p = 7.05 MeV are taken from ref.22. The other data are obtained from tandem Van de Graaff accelator of Kyoto University[25].

Fig. 7. Angular distributions for higher excited states of the reaction $^{12}C(\tau, d)^{13}N$ at 81.4 MeV energy.

References

1) H.T. Fortune, T.J Gray, W. Trost and N.R. Fletcher;
Phys. Rev. 179 (1969) 1033
H.E. Wegner and W.S. Hall; Phys. Rev. 119 (1960) 1654

2) P.S. Hauge; Nuclear Phys. A223 (1974) 394

3) For example;
R.M. Drisko and G.R. Satchler; Phys. Letters 9 (1964) 342
F.G. Perey and D.S Saxson; ibid 10 (1964) 107
J.K. Dikens, R.M. Drisko, F.G. Perey and G.R. Satchler;
ibid 15 (1965) 337

4) For example;
F.C. Hielbert, E. Newman and R.H. Bassel; Phys. Rev. 154 (1967) 898
R.H. Bassel; Phys. Rev. 149 (1966) 791

5) H. Doubri, D. Doyer, M. Arditi, L. Bimbot, N. Frascaria, J.P. Garron and M. Diou; Phys. Letters 29B (1969) 355

6) R. Huby and J.R. Mines; Rev. Mod. Phys. 37 (1965) 406

7) C.M. Vincent and H.T. Fortune; Phys. Rev. C2 (1970) 782

8) K. Yagi, H. Ogawa, Y. Ishizaki, T. Ishimatsu, J. Kokame and K. Matsuda;
Nucl. Instr. 52 (1967) 29

9) J. Kokame and H. Ogata; INS-Technical Report 120 (1972)
(Institute for Nuclear Study, Tokyo)

10) For example;
H.L. Jackson and A.I Galonsky; Phys. Rev. 89 (1953) 370
E.A. Mine; ibid 93 (1954) 762
C.W. Peich, G.C. Phillips and J.L. Russell; ibid 104 (1956) 143
A.C.L. Bernard, J.B. Swint and T.B. Clegg; Nuclear Phys. 86 (1966) 130
E.M. Bernstein and G.E. Terrell; Phys. Rev. 173 (1968) 938

H.O. Meyer; Nuclear Phys. A199 (1973) 413

11) P.D. Kunz; COO-535-606
(University of Colorado 1967)

12) H. Yoshida; DWBA code DWBA4 unpublished

13) H. Collard, R. Hofstader, A. Johansson, R. Parks, M. Reynold, A. Walker and M.R. Vearian; Phys. Rev. Letters 11 (1963) 132

14) G. Puhamel, L. Marcus, H. Langerin-Jobiot, J.P. Didelez, P. Narboni and C. Stephan; Nuclear Phys. A174 (1971) 485

15) K. Koyama, T. Tanabe, M. Yasue, H. Yokomizo, K. Sato, J. Kokame, N. Koori and S. Tanaka; INS-Annual Report (1974) 23
(Institute for Nuclear Study, Tokyo)

16) M. Kawai, K. Kubo and H. Yamaura; INS-PT-9 (MANUAL-2) (1965), revised by M. Igarashi, M. Kawai, K. Kubo and S. Okai

17) W.R. Coker and G.W. Hoffmann; Z. Physik 263 (1973) 179

18) J.L. Yentema and H. Ohnuma; Phys. Rev. Letters 19 (1969) 1341
H. Ohnuma, T. Suehiro, M. Sekiguchi and S. Yamada;
J. Phys. Soc. Japan 36 (1974) 1236

19) T. Udagawa; Private communication

20) J.P. Schiffer, G.C. Morrison, R.H. Siemssen and B. Zeidman;
Phys. Rev. 164 (1967) 1274
S.E. Darder; Nuclear Phys. A208 (1973) 77

21) S.J. Moss and W. Haeberli; Nuclear Phys. 72 (1965) 417

22) G.G. Shute, D. Robson, V.R. Mckenna and A.T. Berztiss; Nuclear Phys. 37 (1962) 535

23) T. Sebe; Prog. theor. Phys. 30 (1963) 290

24) O. Mikoshiba, T. Terasawa and M. Tanifuzi; Nuclear Phys. A168 (1971) 417

25) K. Koyama, N. Matsuoka, H. Sakaguchi and S. Takeuchi;
Private communication

Table 1 Optical potential parameters for ^{3}He and deuteron and binding potential parameters for proton.

	V_0(MeV)	r_0(fm)	a_0(fm)	W_D(MeV)	r_D(fm)	a_D(fm)	V_S(MeV)	r_S(fm)	a_S(fm)	r_C(fm)
$\tau + {}^{12}C$ 1)	118.2	1.00	0.804	14.26	1.17	0.81	——	——	——	1.25
2)	98.9	1.20	0.728	17.0	1.20	0.70	——	——	——	1.25
$d + {}^{13}N$	61.53	1.25	0.667	10.57	1.10	0.84	——	——	——	1.25
$p + {}^{12}C$	adjusted	1.25	0.65	——	——	——	5.5	1.25	0.65	1.25

Table 11 Spectroscopic factors obtained by various calculations discussed in the text.

final state	lj	ZR-L	ZR-NL	LEA-NL	FR-NL	ZR-L (Resonant F.F.)	LEA-NL (Resonant F.F)	Fortune a)	θ_p^2 b)
0	p1/2	0.63	0.63	0.56	0.78	———	———	0.70-1.48	———
2.37	s1/2	0.06	0.08	0.13	0.19	0.09	0.15	———	0.54
3.55	d5/2	0.61	0.72	0.54	0.76	1.13	0.87	———	0.21

a) From ref.1

b) The ratio of proton width to the single particle width (from ref. 3)

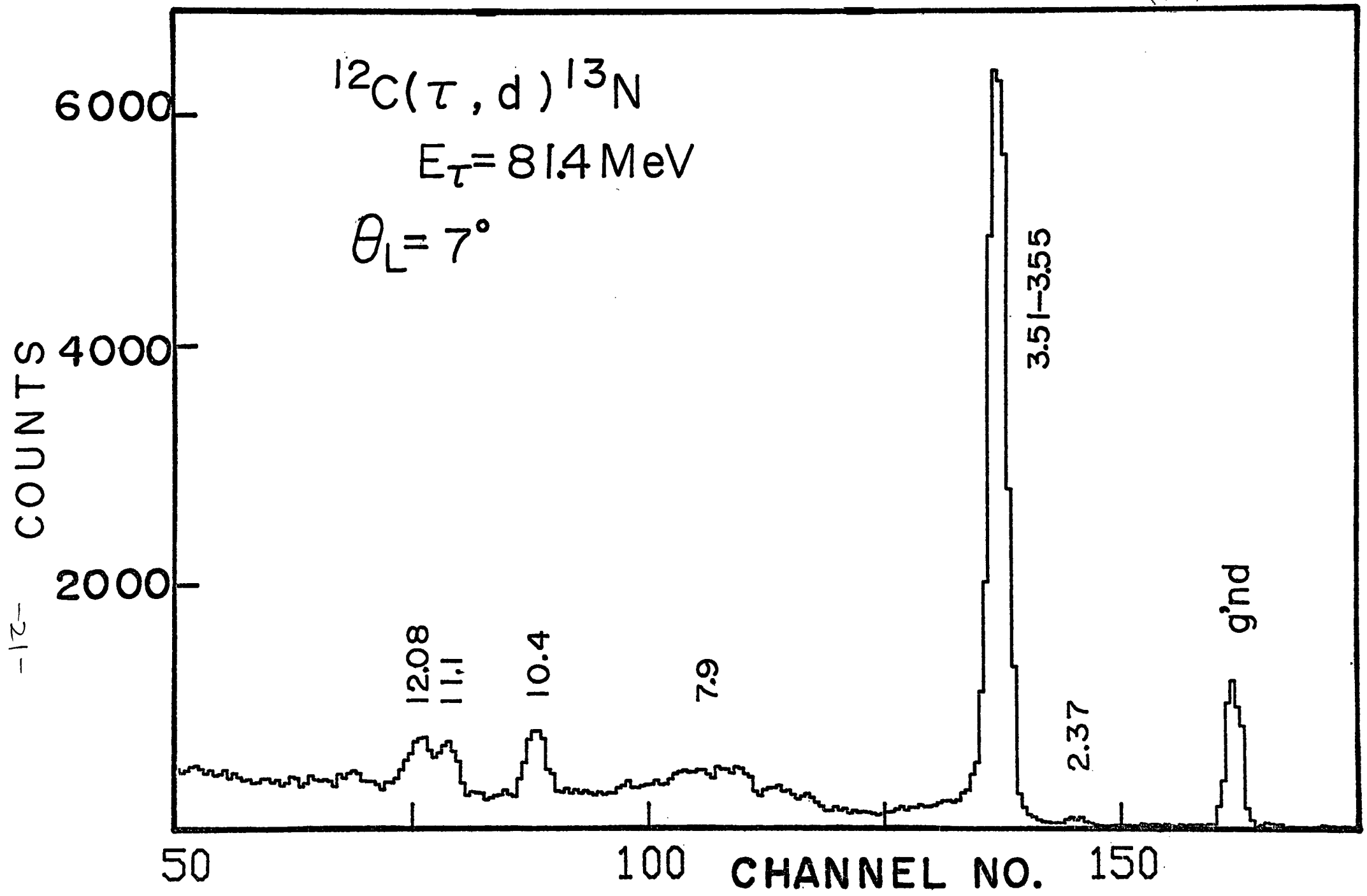
$^{12}C(\tau, d)^{13}N$
$E_\tau = 81.4$ MeV
$\theta_L = 7°$
6000
4000
2000
COUNTS
12.08
11.1
10.4
7.9
3.51–3.55
2.37
g'nd
50
100
150
CHANNEL NO.

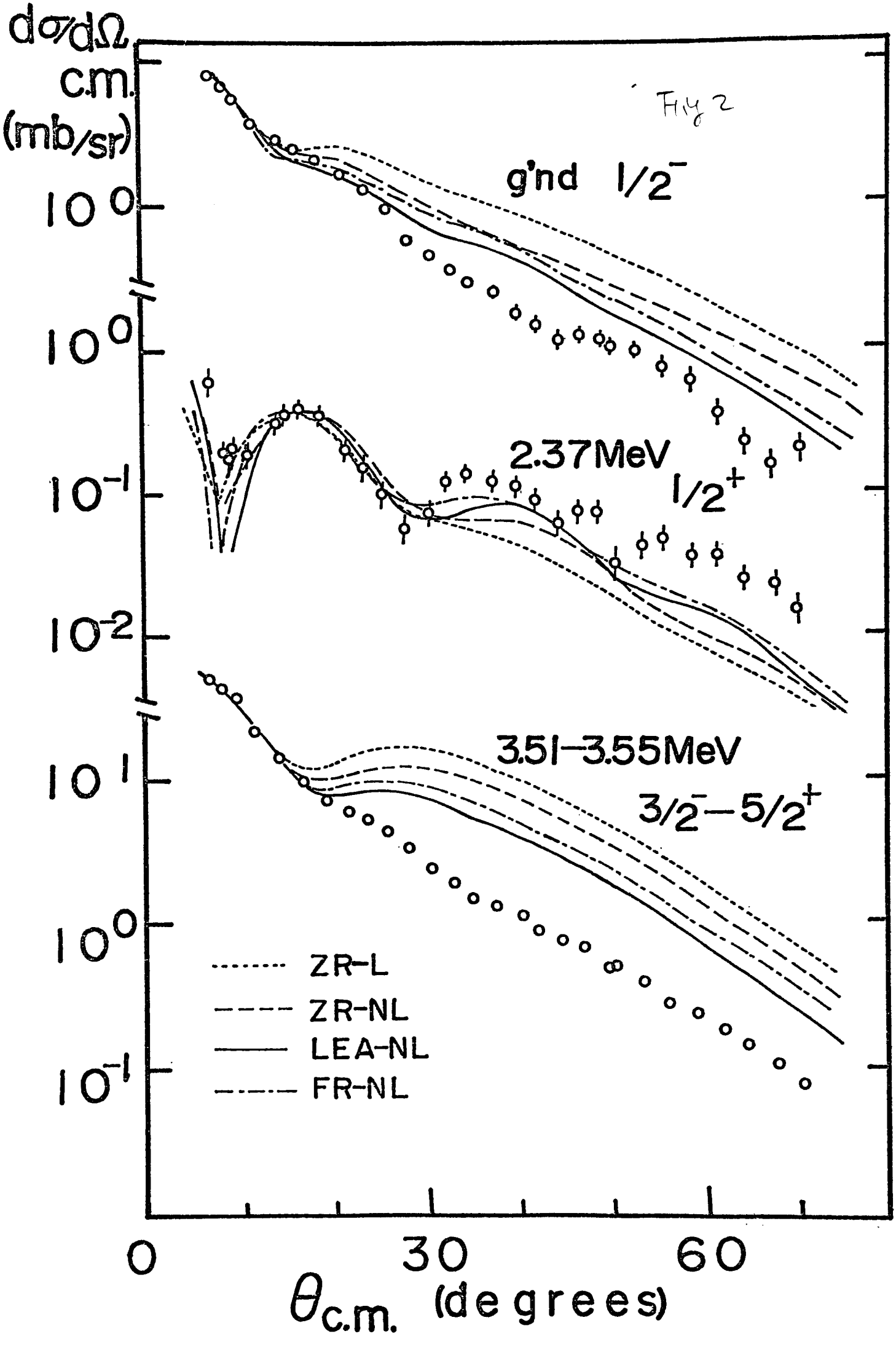
dσ/dΩ c.m. (mb/sr)
Fig 2
g'nd 1/2⁻
2.37MeV 1/2⁺
3.51–3.55MeV
3/2⁻–5/2⁺
ZR-L
ZR-NL
LEA-NL
FR-NL
10 0
10 0
10⁻¹
10⁻²
10 1
10 0
10⁻¹
0
30
60
θc.m. (degrees)

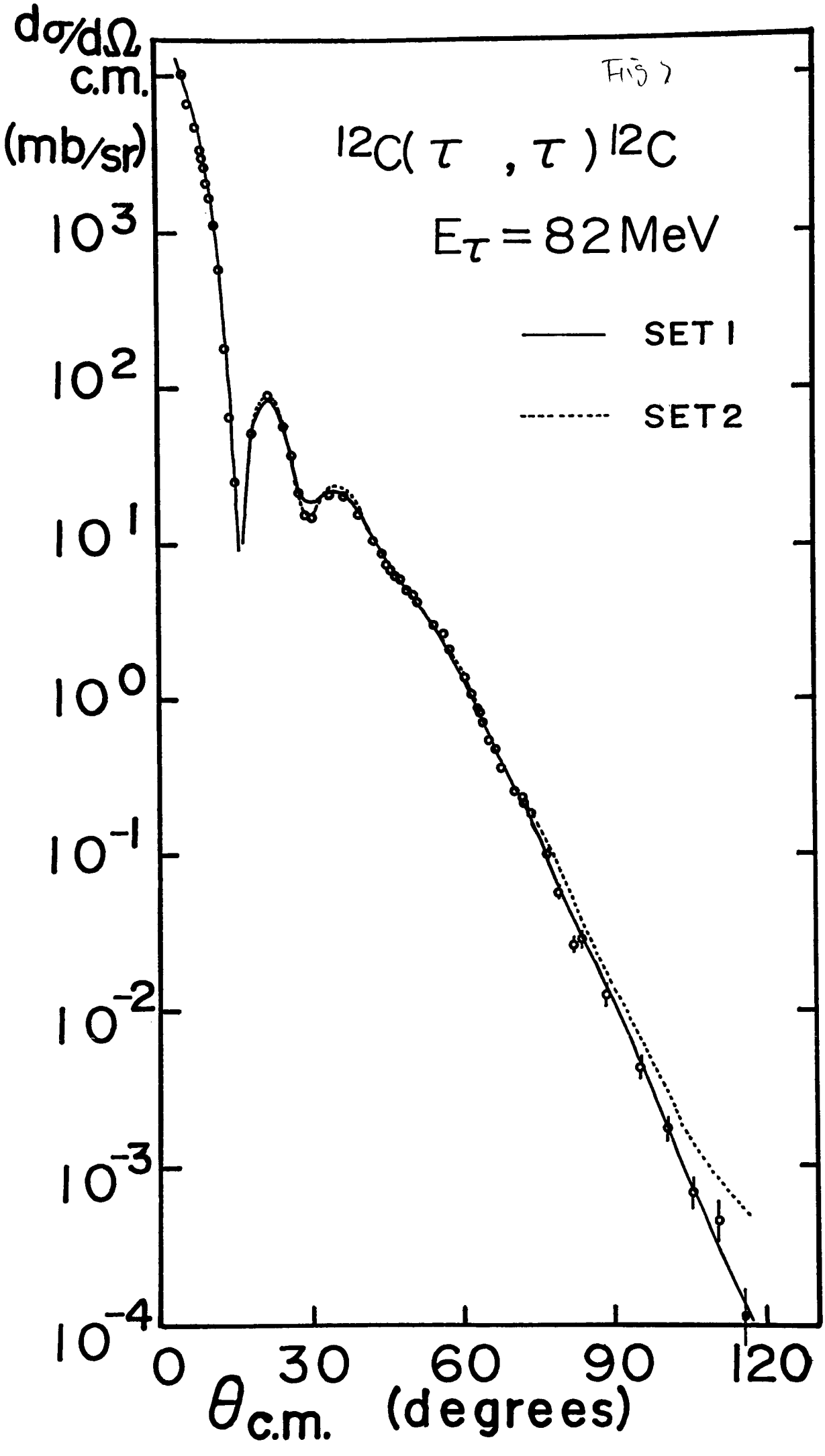
dσ/dΩ c.m. (mb/sr)
FIG 7
$^{12}C(\tau,\tau)^{12}C$
$E_\tau = 82$ MeV
SET 1
SET 2
10^3
10^2
10^1
10^0
10^{-1}
10^{-2}
10^{-3}
10^{-4}
0
30
60
90
120
$\theta_{c.m.}$ (degrees)

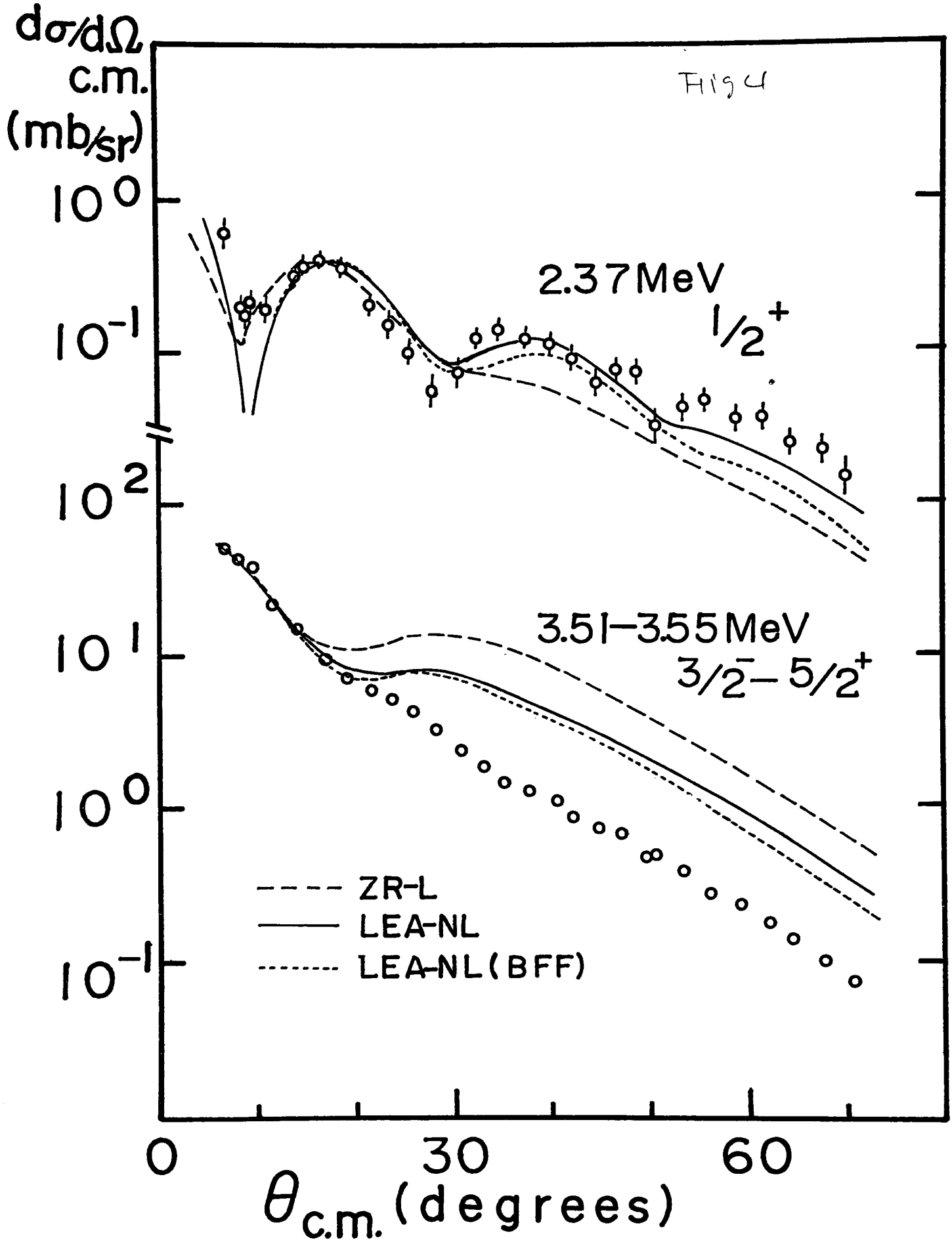
Fig 4
dσ/dΩ c.m. (mb/sr)
10^0
10^-1
10^2
10^1
10^0
10^-1
2.37MeV
1/2+
3.51–3.55MeV
3/2−–5/2+
ZR-L
LEA-NL
LEA-NL(BFF)
0
30
60
θc.m.(degrees)

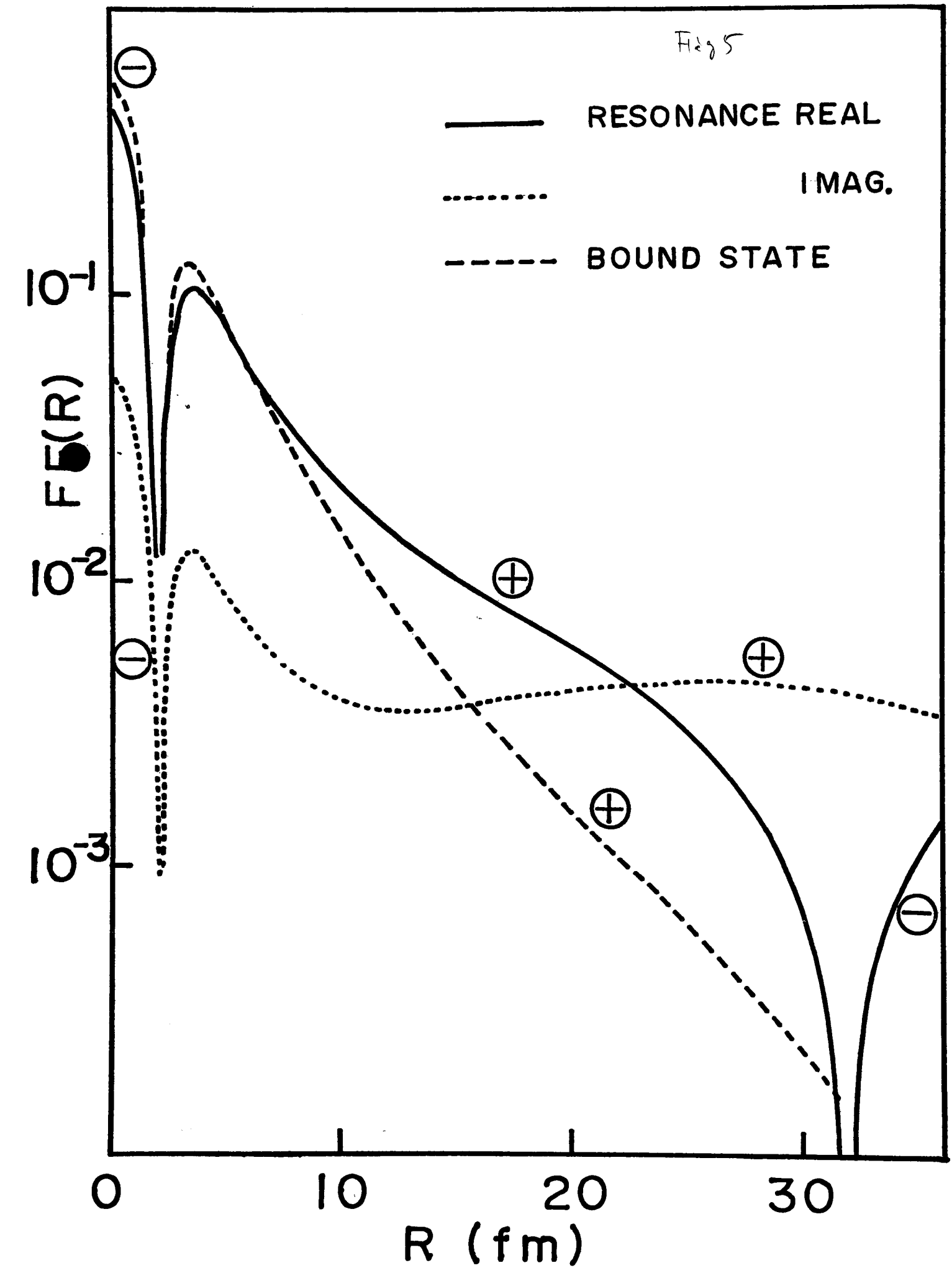
Fig 5
RESONANCE REAL
IMAG.
BOUND STATE
10^{-1}
10^{-2}
10^{-3}
F(R)
0
10
20
30
R (fm)

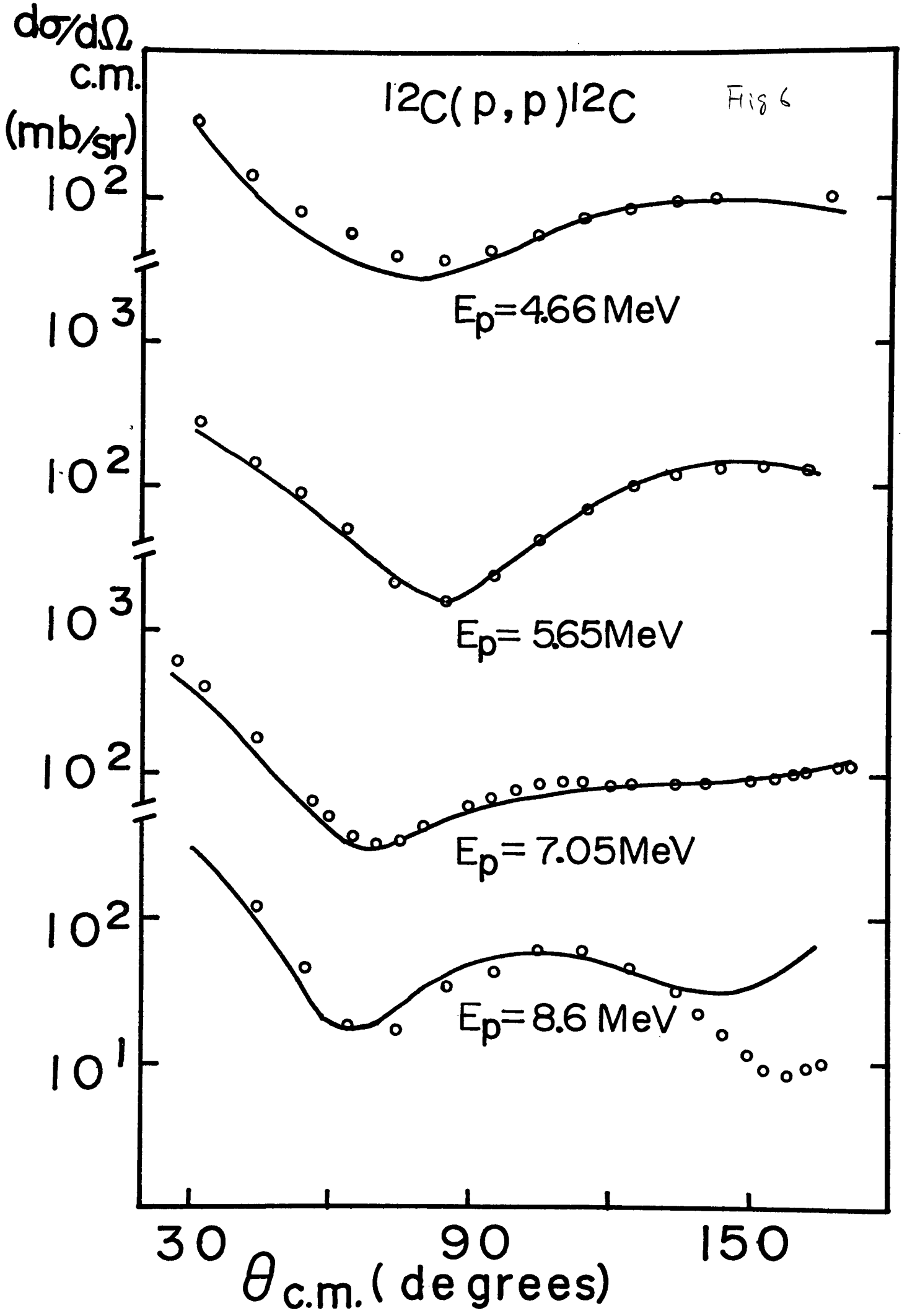
dσ/dΩ c.m. (mb/sr)
12C(p,p)12C
Fig 6
10 2
10 3
Ep=4.66 MeV
10 2
10 3
Ep= 5.65MeV
10 2
Ep= 7.05MeV
10 2
10 1
Ep= 8.6 MeV
30
90
150
θ c.m. (degrees)

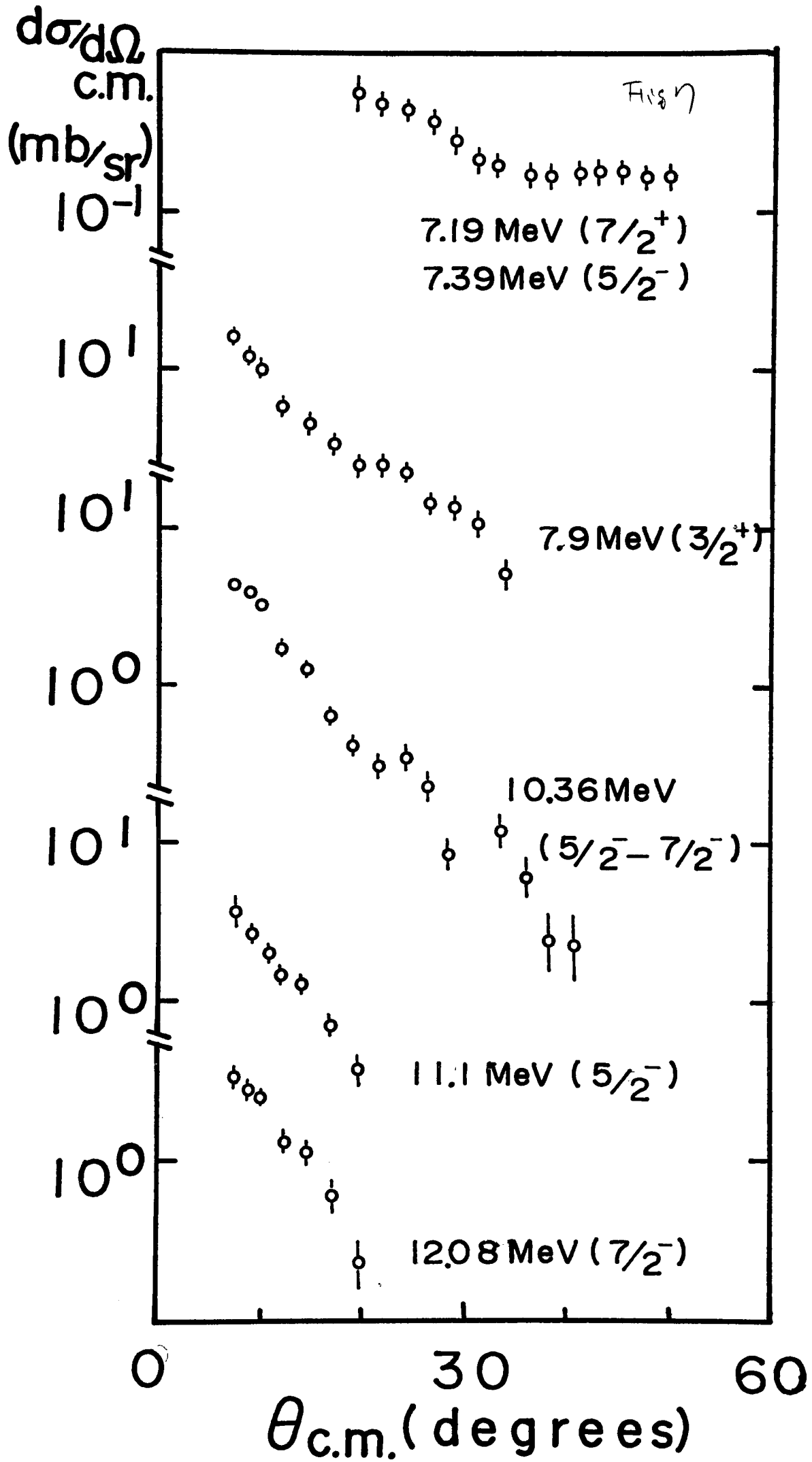
dσ/dΩ c.m. (mb/sr)
10⁻¹
10¹
10¹
10⁰
10¹
10⁰
10⁰
7.19 MeV (7/2⁺)
7.39 MeV (5/2⁻)
7.9 MeV (3/2⁺)
10.36 MeV
(5/2⁻ – 7/2⁻)
11.1 MeV (5/2⁻)
12.08 MeV (7/2⁻)
0
30
60
θc.m. (degrees)